

**Review Article: Review of electrohydrodynamical ion sources and their applications to focused ion beam technology**

Gierak, J.; Mazarov, P.; Bruchhaus, L.; Jede, R.; Bischoff, L.;

Originally published:

October 2018

**Journal of Vacuum Science & Technology B 36(2018)6, 06J101-1-06J101-6**

DOI: <https://doi.org/10.1116/1.5047150>

Perma-Link to Publication Repository of HZDR:

<https://www.hzdr.de/publications/Publ-28088>

Release of the secondary publication  
on the basis of the German Copyright Law § 38 Section 4.

# Review of Electro-Hydro-Dynamical ion sources and their applications to Focused Ion Beam technology

J. Gierak <sup>a)</sup>

Centre de Nanosciences et de Nanotechnologies (CNRS - Université Paris-Sud) Route de  
Nozay, Marcoussis - France

P. Mazarov, L. Bruchhaus, and R. Jede

Raith GmbH - Konrad-Adenauer-Allee 8 - 44263 Dortmund – Germany

L. Bischoff

Helmholtz-Zentrum Dresden-Rossendorf, Institute of Ion Beam Physics and Materials Research,  
Bautzner Landstrasse 400, 01328 Dresden, Germany

<sup>a)</sup> Electronic mail: jacques.gierak@c2n.upsaclay.fr

In this article we review, compare and discuss the characteristics and applicative potential of a variety of non-Gallium ion Liquid Metal Ion Sources (LMIS) we have developed and successfully applied to nano-patterning. These sources allow generating on-demand ion beams and are promising for extending Focused Ion Beams (FIB) applications. We detail the operating characteristics of such sources capable to emit metal projectiles ranging from atomic ions with different charge states, to poly-atomic ions and to large metal clusters having sizes up to a few nanometers. We highlight their interest and relevance to current nanoscience challenges in terms of ultimate patterning or bottom-up nanofabrication capabilities.

## I. INTRODUCTION

In the pursuing quest aiming at unveiling the full applied potential of the robust, well-established and successful direct-write Focused Ion Beam (FIB) technology, there has been a major effort invested around the world aiming at developing alternative ion sources to Ga LMIS. Gallium LMIS were at the origins of FIB technology and remain very appreciated and widely used for application ranging from inspection to rapid prototyping of research devices or strategic components at a small fraction of the \$5 million to \$10 million in costs that are typical for a new lot of wafers or masks in a factory <sup>1</sup>. Nowadays Gallium-based FIB systems are intensively used by the semiconductor industry where this technology allows routine or even automated circuit edit, failure analysis so that designers can cut connections or add metal straps within a precisely identified chip.

Alternative ion sources to Ga-LMIS can be found with the Helium or Neon Gas Field Ion Sources (GFIS) <sup>2</sup>. This GFIS based instrument developed initially with the aim of performing advanced ion microscopy, with a close to atomic level imaging capability, has been rapidly applied against some nano-patterning challenges with a great success. Indeed a GFIS emission is based on an atomic-sized emitter of very high brightness ( $B > 4.10^9$  A/cm<sup>2</sup>.sr for an He GFIS) and thus is capable to deliver much smaller spot sizes (0.25nm for an He GFIS) in comparison with Ga-LMIS. On the other hand because of available GFIS probe currents (pico-Ampère sized) and lower ion atomic masses, higher

ion fluences are required to achieve significant sputtering effect; a parameter of the highest importance for a vast majority of FIB users<sup>3</sup>.

On the other side of the ion source arsenal, as a response to the FIB main market persistent demand, i.e. the IC edit community, asking for erosion speeds in excess of 500  $\mu\text{m}^3/\text{s}$ ) for large volume milling of IC packaging structures, 3D-IC's / Interconnects and delayering of IC's, inductively coupled plasma sources were proposed and developed<sup>4</sup>. These plasma sources do not exhibit brightness values as high as GFIS or even LMIS (typically two orders of magnitude lower than a Ga-LMIS), but they allow FIB machining with probe currents up to the micro-Ampère and therefore allow high etching speeds and large volume removal. Additionally low sample contamination and strong localized ion energy deposition when heavy ion species such as Xenon are used.

More recently ion sources based on ionization of laser cooled atoms have been investigated and successfully applied to FIB instruments<sup>5</sup>. The production of reactive ionic species such as Cesium ions could allow significant improvements in resolution down to about 2 nm and throughput in some applications such as IC circuit edit and high resolution Secondary Ion Mass Spectrometry (SIMS).

Nevertheless as a complement to high current ion sources or atomic-sized ion emitters, high performance Liquid Metal Ion Sources and Liquid Metal Alloys Ion Sources exhibit definitive advantages at the prototyping level. Indeed their still remarkable brightness ( $B \sim 2 \cdot 10^6 \text{ A/cm}^2 \cdot \text{sr}$  for a Ga-LMIS), excellent emission stabilities (current emission fluctuations and emitting area invariance) resulting in probe current variations well below 0.5% per hour. Their costs of ownership, operation and maintenance are by far the lowest of all the sources considered here. Finally their simplicity of operation and their extended lifespan from several hundreds of hours for sources requiring a heating to thousands (years of operation) remain chief's arguments. With this respect, one should note the considerable amount of efforts that has been invested in recipes, precursor gas chemistry to achieve either enhanced Gas-Assisted Etching (GAE) or Gas-Assisted Deposition (GAD) to extend primarily the Ga-FIB technique. With the introduction of reactive chemical precursors it is possible to enhance FIB etching effect on selected regions, depose metal containing layers or insulating materials on specific areas in order to repair masks, or modify integrated circuits.

## II. EXPERIMENTAL

Although there is a very large number of metallic ion species available to LMIS and therefore to FIB applications one should note that gallium remains the most used element. Gallium has some interesting and unique characteristics in terms of a low melting point, low vapor pressure, excellent compatibility and wetting properties of tungsten that is used for tip fabrication or hairpin filaments. Therefore the coupling of this simple and efficient setup with a charged particle optics has led to the emergence of FIB technology<sup>6</sup>.

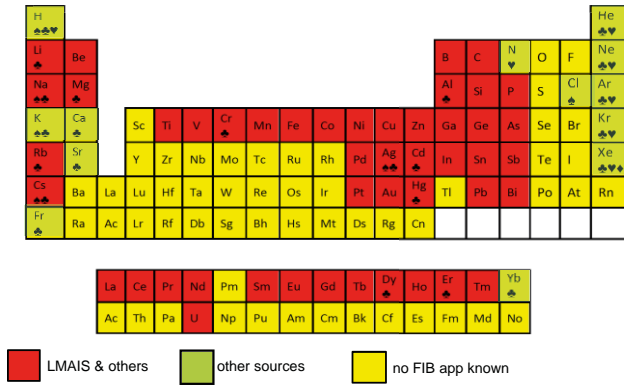


FIG. 1. Periodic table of elements showing the different ionic species available from LMIS / LMAIS (Red) and of alternative ion sources (Green: ILIS ♠, MOTIS ♣, GFIS ♥, Xe-FIB ♦)

Very early and intensive effort has been initiated to propose alternative metals extending LMIS to ion species other than Ga and for example to allow semiconductor dopant implantations by switching N to P dopants emitted from a same Liquid Metal Alloy Ion Source (LMAIS) <sup>7</sup>. This opens some possibilities from the need to select suitable ion species to non-doping or sample or processing friendly for a better control of ion induced contamination, to selective implantation of ion species or particle deposition. To this end, an effort aiming at extending the LMIS to other metals and alloys has been maintained over the years, expanding the possibility to as many as 46 different ionic species, (Figure 1) either from pure metals or alloys. Many elements can be produced from eutectic alloys as a global beam containing ion species from each alloy constituent. At this point one should mention that all these alloy sources require a mass separating functionality to be inserted in the ion focusing and transport optics, adding to a moderate system complexity but allowing the access to most of the periodic table elements.

### A. Aluminum and Gold metal LMIS

We have developed an Aluminum LMIS that has the advantage of offering a relatively light ion; Aluminum has a melting point around 600°C, a low vapor pressure, a high surface tension promoting viscous wetting behavior on the emitter needle. It is in particular very promising for high resolution FIB applications since it has only one isotope. In addition for IC edit aluminum is not considered, in most cases, as a contaminant. The drawback is that Al reacts and corrodes W wires readily. Our approach is aiming at substituting LMIS tip and reservoir material with carbon material together with a suitable adhesion layer (Figure 2) <sup>8</sup>. The lower beam divergence of the emitted Al+ beam coupled with a FIB accounts for an increased beam current density and keeps etching speeds comparable to gallium in particular on III-V materials. Selective and stable damage implantation of Aluminum ions allows stable patterning like Multi Quantum Wells (MQWs).

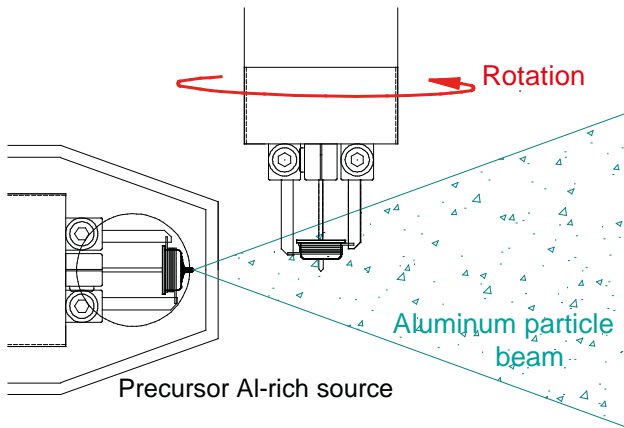
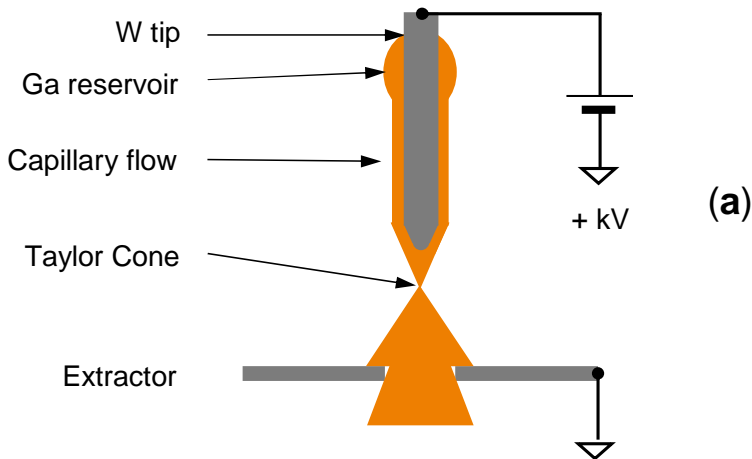


FIG. 2. Schematic of the irradiation setup used to deposit and insert an aluminum wetting layer into the graphite tip and reservoir. This irradiated tip is then immersed in a molten aluminum and only the irradiated surface is filled with aluminum.

Gold with a higher melting point ( $\sim 1000\text{ }^{\circ}\text{C}$ ) also exhibits good performances on LMIS applications. This is mainly due to its very high diffusivity on a Tungsten metal tip or reservoir, thus allowing to reduce stable emission current limits well beyond Ga-LMIS standards ( $< 0.1\text{ }\mu\text{A}$ ). Gold focused Ion Beams can be used to insert inside a target crystal catalyst gold particles without any contamination caused by lithographical processes based on resists. This allows the epitaxial growth of very high aspect ratio nanowires (NWs) of GaAs or GaN.



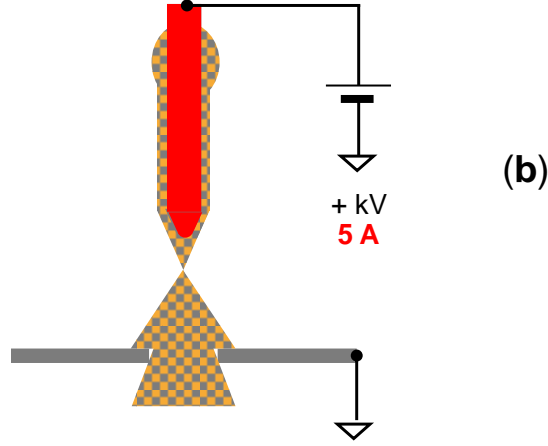


FIG. 3. Schematic of the differences between a Ga-LMIS (a) where no heating current is required to melt the supply metal and a LMAIS (b) filled with an eutectic alloy requiring the tip to be heated with a 5 Amps current to allow ion emission of both ion species.

It is also interesting to note that this technology has the potential to be extended down to the so-called “Atomic Sized Ion Source” with the emission of gold ions field evaporated from the apex of a reconstructed gold nanostructure at needle apex. This is achieved by reducing the gold film temperature and avoiding a Taylor cone formation by allowing only surface diffusion of a few gold atoms at a time<sup>9</sup>.

## B. Alloy LMAIS

For specific purposes like high resolution Focused ion beam implantation or focused ion beam induced ion mixing, other ions than gallium are needed. Therefore we have developed Liquid Metal Alloy Ion Sources (LMAIS) to match some application area. Hereafter we present our results in terms of:

### B.1. Light Ions for high precision fabrication and imaging resolution at the 2 nm level.

Crucial parameters of an LMIS are the energy spread  $\Delta E \sim I^{2/3} m^{1/3} T^{1/2}$  and the virtual source size  $d_v \sim (m^{1/2} I)^{0.45}$  (i.e.: the disk from where the ions seem to come from), due their influence to the final spatial resolution of a FIB system ( $T$  is the temperature of the source,  $m$  is the mass of the ions and  $I$  is the emission current)<sup>7</sup>. The predicted dependence of both parameters on the mass of the ions presumes to use of light ions to get high beam resolution. The lightest ions delivered by a LMAIS are Li, Be, B and C. The deleterious handling and technological source production difficulties are main disadvantages of sources with all these materials. To overcome these problems suitable alloys were chosen for desirable ions, which in combination with different source/tip material brings a long term stability of the beam current over many hours. As an example the high voltage stability, set to 35 kV, as well as the emission current set to 3.0  $\mu\text{A}$  is shown in Fig. for an  $\text{Au}_{68}\text{B}_5\text{Ge}_{22}\text{Ni}_5$  (the most stable alloy for B ions) LMAIS in a ionLINE IONselect system (Raith GmbH) over a duration of about 60 hours in a second clock cycle. An  $\text{Au}_{70}\text{Si}_{15}\text{Be}_{15}$  LMAIS can deliver doubly charged Be ions with high intensity and therefore can be used for local doping of III-V semiconductors. Another element of interest is AlCCe for generating a small beam spot size focused carbon ion

beam <sup>10</sup>. This availability of a carbon ion source opens up many new applications in graphene research as well as in FIB applications involving organic materials.

Li containing LMAIS, in particular Li and Ga<sub>35</sub>Bi<sub>60</sub>Li<sub>5</sub> sources with predicted smallest energy spread for Li of about 2 eV are described in detail in <sup>11</sup>. A new promising solution was found by introducing 10% of Li into a stable working In<sub>67</sub>Bi<sub>33</sub> alloy with a melting point of only 90°C. The mass spectrum of the final In<sub>60</sub>Bi<sub>30</sub>Li<sub>10</sub> LMAIS is shown in Fig.4. Bi is the heaviest, not radioactive element and thus best suited for high rate sputtering.

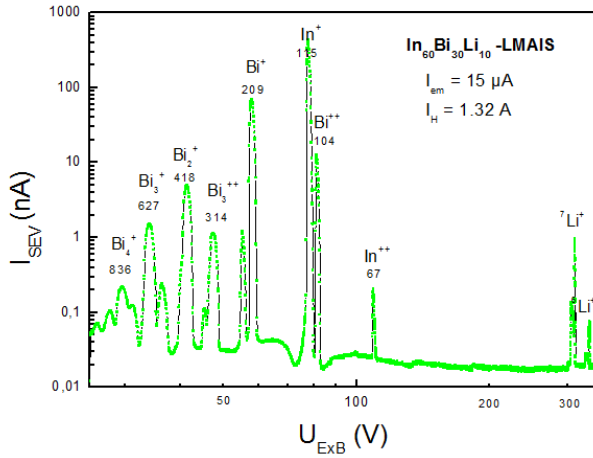


Fig. 4. Mass spectrum of an In<sub>60</sub>Bi<sub>30</sub>Li<sub>10</sub> LMAIS obtained with  $I_{em} = 15 \mu A$ .

### B.2. Polyatomic Projectiles generation

The use of Au<sub>n</sub><sup>k+</sup>, Bi<sub>n</sub><sup>k+</sup>, Pb<sub>n</sub><sup>k+</sup> (n = 1–7, k = 1,2) atoms and cluster ion projectiles allow very localized and important localization that dramatically enhances the sputtering yield of target materials and therefore allow precise substrate delayering. The non-linear sputter effects induced by cluster bombardment give additional a milling enhancement. Furthermore, the roughness induced by the cluster projectile impact is much less pronounced than that generated by the atomic projectiles Ga<sup>+</sup> and the penetration depth is smaller, leading to less contamination and amorphisation of the target.

B. 3. Ion species for localized FIB implantation: Co<sup>++</sup> ions were used for a local ion beam synthesis of CoSi<sub>2</sub> nanostructures down to 20 nm after annealing <sup>12</sup>.

### C. Liquid Metal Cluster Source - LMCS

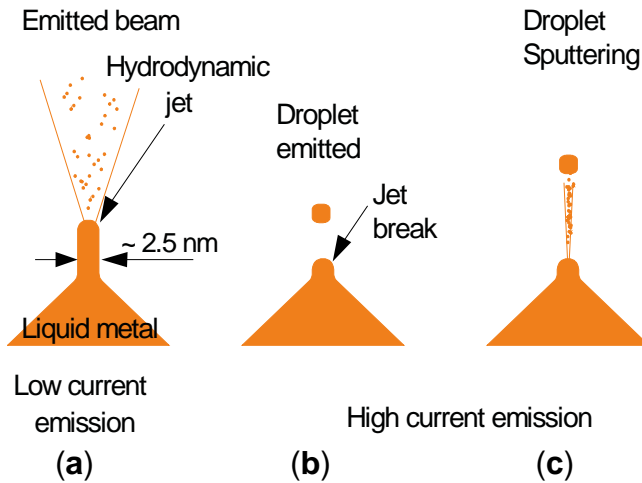


FIG. 5.a. Schematic of LMIS / LMAIS apex for low current emission ( $< 15 \mu\text{A}$ ). (b) Apical jet fragmentation during operation at high current emission ( $\sim 50 \mu\text{A}$ ) allowing charged droplet creation (c) In flight droplet fragmentation by resuming emitted fast ions.

In this section we present our original deposition methodology in which the incoming species are small droplets emitted by a Gold LMIS, we operate in a high emission current regime ( $> 40 \mu\text{A}$ ). At this high emission current the protruding jet at Taylor cone apex is elongated close to a maximum extend fixed by the metal surface tension and the pressure of the liquid flow inside the meniscus<sup>13</sup>. Above this limit the jet is ruptured and jet fragment are reproducibly emitted as metal clusters retaining the dimension of the naometer-sized emitting jet, see Figure 5. The mechanism can be described as follow:

The end of the liquid protrusion breaks to form a droplet of a similar radius to the protrusion,

This droplet is accelerated by the electrostatic field and for a certain time interval the emission is shut off due to the screening effect of the accelerating droplet,

Emission restarts when the screening becomes negligible.

### III. RESULTS AND DISCUSSION

#### A. Imaging

The use of light ions such as  $\text{Li}^+$ ,  $\text{Be}^{++}$ ,  $\text{B}^+$ ,  $\text{C}^+$ ,  $\text{Si}^{++}$  or even  $\text{Al}^+$  allows definitive advantages in Scanning Ion Microscopy using classical FIB.



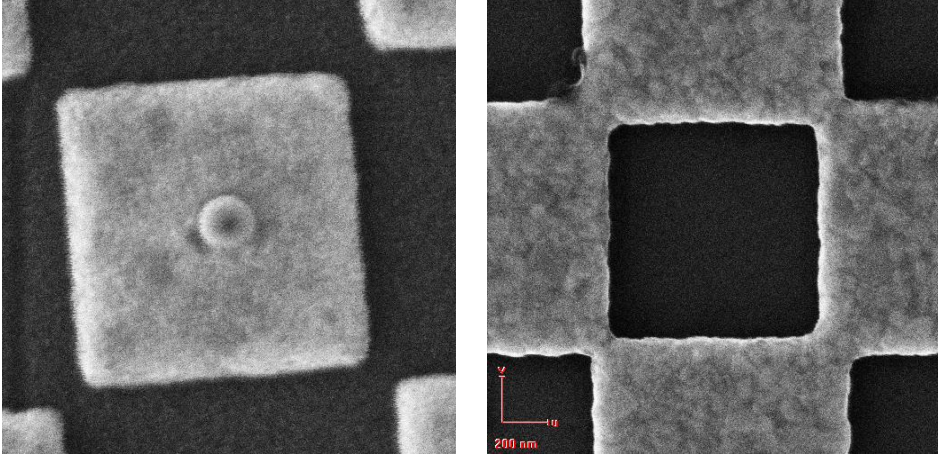


Fig.6. (a) Secondary electron images generated by a scanning  $\text{Li}^+$  (35 keV) and (b)  $\text{Be}^{++}$  (70 keV) ion beam of  $1 \mu\text{m}$  gold squares on silicon.

### B. Implantation

FIB implantation of cobalt can be applied to form  $\text{CoSi}_2$  patterns using a  $\text{Co}_{36}\text{Nd}_{64}$  LMAIS allowing ion beam synthesis for creating interconnects<sup>14</sup> into silicon substrates. Implantation can be performed in polysilicon, amorphous and crystalline silicon at room temperature with subsequent annealing at  $600^\circ\text{C}$  for 1 h. The implantation dose required must be high enough to induce the formation of a continuous layer with a critical incident ion dose of about  $8 \cdot 10^{16}$  ions/ $\text{cm}^2$ .

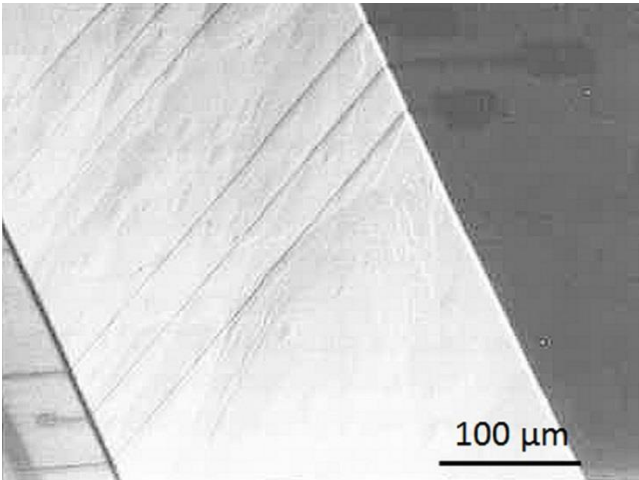


Fig 7. 35 keV  $\text{Co}^+$  FIB implanted interconnects between the top surface and the bottom of a  $200 \mu\text{m}$  deep etch groove in Si at  $400^\circ\text{C}$ , then transformed to  $\text{CoSi}_2$  after a  $600^\circ\text{C} + 1000^\circ\text{C}$  annealing.

Focused ions beams can also be used for localized epitaxy of semiconductor nanowires Using a Gold ion beam it is possible to realize array of dots implanted with gold ions. For ion doses around  $10^6$  ions/dot of 20 keV gold ions on a  $\langle 111 \rangle$  GaAs samples it is possible to form gold islands at the surface. Then UHV VLS nanowire

growth is achieved in a second step into a MBE III-V growth system. Stable NWs, very high aspect ratio and highly crystalline structures can be obtained that remain very challenging to fabricate using classical lithographical processes based on resists<sup>15</sup>.

Stable magnetic structures can also be written directly using appropriate ions. In Fe–Cr films the metastable paramagnetic phase can be transformed into a more stable BCC phase which is ferromagnetic. Such a ferromagnetic pattern was written by a fine-focused Cr-ion beam in a paramagnetic alloy (face-centred orthorhombic, 37 at% Cr) using an alloy LMIS ( $\text{Er}_{70}\text{Fe}_{22}\text{Ni}_5\text{Cr}_3$ ) and could be detected by magnetic force microscopy<sup>16</sup>.

### **C. Surface processing**

Heavy ions or poly-atomic ion  $\text{Bi}_n^{m+}$  irradiation of Ge at RT results in a self-organized well-ordered hexagonally dot pattern due to the high energy deposition by the heavy polyatomic projectiles<sup>17</sup>. Irradiation with heavy mon- or polyatomic ions like  $\text{Bi}_n^{m+}$ ,  $\text{Au}_n^{m+}$ ,  $\text{Pb}_n^{m+}$  of Ge at RT results in a self-organized surface pattern depending on the angle of incidence due to the high energy deposition by the heavy projectiles<sup>16</sup> as shown on Figure 8. In the case of high angle irradiation attended by a ripple structure formation the erosion rate is decreased due to the wide variety of surface angles faced to the beam

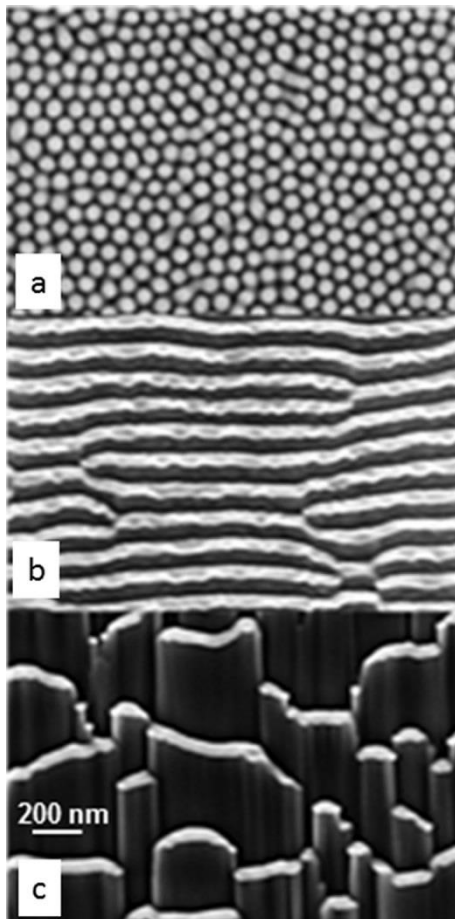


Fig. 8. Pattern evolution for  $\text{Bi}_3^{++}$  polyatomic ion irradiation of Ge ( $D= 5.10^{16} \text{ cm}^{-2}$ , 30 keV) at room temperature as a function of angle of incidence. a) regular hexagonal dot pattern at normal incidence, b) ripple structure formation at  $75^\circ$  and c) shingles at  $85^\circ$ .

#### D. Clusters deposition

Using a Gold LMIS sub-2 nm clusters can be generated, transported and deposited at selected places. Adjusting the particle energy by controlling the emission tip voltage down to 1 kV allows a precise control of the cluster landing energy and limit their fragmentation at impact. Under optimized conditions the average size of the islands deposited can be close to 1 nm, and there are no traces of coalescence between islands demonstrating that the surface diffusion of the gold deposited particles islands is limited by this energetic insertion process<sup>18</sup>. Using the FIB technique Au islands can be deposited between contact electrodes and allow to realize devices like Multi Tunnel Junction devices (Figure 9), exhibiting Coulomb blockade effects observed up to a temperature of 200 K and charging energy estimated around 240 meV.

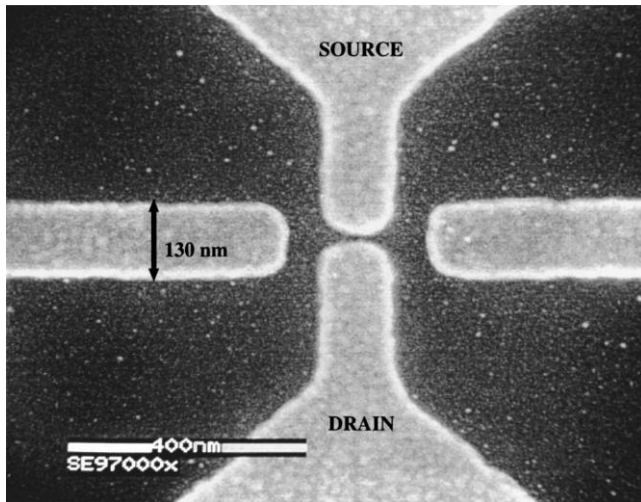
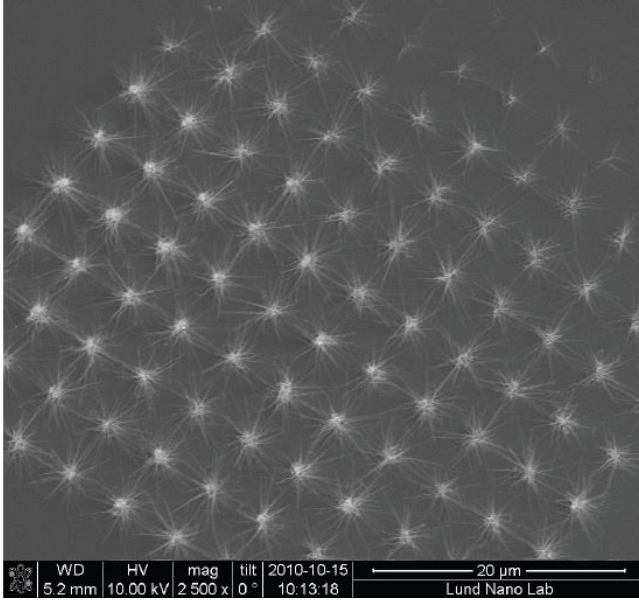


Fig.9. Scanning electron microscopy image of a MTJ device after droplet deposition. Source and drain electrodes are the vertical fingers separated by a 10 nm gap. Reprinted with permission from *J. Vac. Sci. Technol. B* 16(6), Nov/Dec 1998, Copyright American Vacuum Society.

Alternatively Gold particles can be used for bottom-up like applications such as localized growth of ultrathin (< 20nm in diameter) gallium phosphide (GaP) nanowires in a controlled manner by combining localized deposition of gold particles to act as a precursor and epitaxy techniques<sup>19</sup>. Below we illustrate on figure 10 the potential of this technique using a GaP sample irradiated using an ion beam energy of 20 kV to realize organized arrays of GaP NWs.



*Fig.10. SEM image of GaP nanowires grown from gold nano-islands deposited in a matrix array with variable dose of Gold particles.*

## IV. SUMMARY AND CONCLUSIONS

The investigation and application of LMIS other than for Ga in terms of alternative pure metal ion sources (LMIS) or alloy sources (LMAIS) used in both conventional and mass-separated FIBs are reviewed. We show that, using these alternative or emerging LMIS/LMAIS, some important challenges for nanosciences can be elegantly addressed using the direct ions writing method. We show that enlarging the very popular FIB technique to these alternative ions is straightforward and keeps in many aspects the native versatility and simplicity of FIB technology. All these LMIS/LMAIS exhibit sufficient brightness, leading edge emission stabilities, and lifespan for successfully addressing many micro- and nano-technology tasks where a broader spectrum of ions and processes is explored.

## ACKNOWLEDGMENTS

The authors thank W. Pilz for his encouragement. The support from the Ion Beam Center (IBC) of the HZDR is gratefully acknowledged. This work has been performed under the cooperation agreement Raith CNRS Nr 162226<sup>20</sup>.

<sup>1</sup> T. Mohiuddin, Electronic Design, Jan 24, 2014.

<sup>2</sup> T. B.W. Ward, J.A. Notte, N. P. Economou, J. Vac. Sci. Technol. B 24, 2871 (2006).

<sup>3</sup> S. Tan, R. Livengood, P. Hack, R. Hallstein, D. Shima, J. Notte and S. McVey, J. Vac. Sci. Technol. B 29, 06F604-1 (2011).

<sup>4</sup> N. S. Smith, W. P. Skoczylas, S. M. Kellogg, D. E. Kinion, P. P. Tesch, O. Sutherland, A. Aanesland and R. W. Boswell, J. Vac. Sci. Technol. B 24, 2902 (2006).

- <sup>5</sup> A.V. Steele, A. Schwarzkopf, J. J. McClelland, B. Knuffman, Nano Futures 1, 015005 (2017).
- <sup>6</sup> R. L. Seliger, J. W. Ward, V. Wang, and R. L. Kubena, Appl. Phys. Lett. 34, 310 (1979).
- <sup>7</sup> L. Bischoff, P. Mazarov, L. Bruchhaus, and J. Gierak, Appl. Phys. Rev. 3, 021101 (2016).
- <sup>8</sup> J. Gierak and G. Ben Assayag, Mic. Eng. 30, 261(1996).
- <sup>9</sup> S. T. Purcell, V. T. Binh and P. Thevenard, Nanotechnology 12, 168 (2001).
- <sup>10</sup> P. Mazarov, A. D. Wieck, L. Bischoff, and W. Pilz, J. Vac. Sci. Technol. B 27, L47 (2009).
- <sup>11</sup> L. Bischoff and Ch. Akhmadaliev, J. Phys. D: Appl. Phys. 41, 052001 (2008)
- <sup>12</sup> Ch. Akhmadaliev, L. Bischoff and B. Schmidt, Mat. Sci. . Engin. C 26, 818 (2006).
- <sup>13</sup> R. Hornsey and T. Ishitani, Japanese Journal of Applied Physics, 29, L1007 (1990).
- <sup>14</sup> J. Teichert, L. Bischoff, E. Hesse, P. Schneider, D. Panknin, T. Geßner, B. Löbner, and N. Zichner, ,Appl. Surf. Sci. 91, 44-49 (1995)
- <sup>15</sup> J. Gierak, A. Madouri, E. Bourhis, L. Travers, D. Lucot, and J.C. Harmand, Microelec. Eng. 87, 1386 (2010).
- <sup>16</sup> G. Gorbunov, A. A. Levin, E. Wieser, L. Bischoff, D. Eckert, A. Mensch, M. Mertig, D. C. Meyer, H. Reuther, P. Paufler, and W. Pompe, Proc. SPIE 5121, 306 (2003).
- <sup>17</sup> L. Bischoff, K.-H. Heinig, B. Schmidt, S. Facsko, and W. Pilz, Nucl. Instr. and Meth. B 272, 198 (2012).
- <sup>18</sup> C. Vieu, A. Pepin, J. Gierak, C. David, Y. Jin, F. Carcenac, and H. Launois, J. Vac. Sci. Technol. B 16(6), Nov/Dec 1998
- <sup>19</sup> G. Piret, H. Persson, M. T. Borgström, L. Samuelson, S. Guilet, A. Morin, E. Bourhis, A. Madouri, C. Prinz and J. Gierak, nanoICT, E-Nano Newsletter n° 25 (2012)
- <sup>20</sup> <https://www.raith.com/news/c2n-cnrs-upsud-and-raith-continue-cooperation-over-advanced-fib-nanofabrication-technologies.html>